Available online at www.sciencedirect.com

SCIENCE DIRECT®

Nuclear Instruments and Methods in Physics Research A 564 (2006) 57–65

NUCLEAR INSTRUMENTS & METHODS IN PHYSICS RESEARCH
Section A

www.elsevier.com/locate/nima

Performance of the upgraded laser system for the Fermilab-NIU photoinjector

Jianliang Li*, Rodion Tikhoplav, Adrian C. Melissinos

Department of Physics and Astronomy, University of Rochester, Rochester, NY 14627, USA

Received 13 December 2005; received in revised form 31 March 2006; accepted 2 April 2006
Available online 4 May 2006

Abstract

The laser system for the Fermilab-NIU photoinjector has been recently upgraded in order to improve reliability and to reduce amplitude fluctuations. Major modifications included the replacement of the oscillator by a diode-pumped passively mode locked Nd:YLF commercial laser. The oscillator delivers 5 ps long pulses at 81.25 MHz at an average power of 450 mW. The number of round trips in the multi-pass amplifier was reduced by half and image relaying was introduced throughout the optical system. The frequency of the IR ($\lambda = 1054$ nm) pulse was quadrupled to UV ($\lambda = 263.5$ nm) by two BBO crystals. The overall efficiency for frequency quadrupling was of order 20%. The shot to shot fluctuations in the UV are ~5%. The UV energy on the cathode is 5 μJ/pulse (10 μJ/pulse without the pulse stacker), yielding charge of 10 nC/pulse.

PACS: 29.17.+w; 41.75.Jv; 42.60.−v

Keywords: RF photoinjector; High energy laser; Linear accelerator

1. Introduction

The Fermilab/NIU photoinjector [1] consists of a photoemission electron source based on an L band RF-gun. The CsTe photocathode is illuminated by an ultrashort (5 ps) UV laser pulse. The gun is followed by a 9-cell superconducting cavity, beam-focusing elements to handle the 14.8 MeV low emittance electron beam and appropriate diagnostics. Beam charge as high as 10 nC/pulse can be delivered. A schematic overview of the photoinjector is shown in Fig. 1. In this paper, we describe the modifications made to the original laser and the performance of the upgraded laser system.

The upgraded laser system is shown in Fig. 2 and is located on two 4 × 8 feet optical tables. The oscillator [2] ($\lambda = 1054$ nm) delivering 450 mW of 5 ps long pulses at 81.25 MHz, is phase locked to the master oscillator that controls the L-band RF. A single pulse is selected out of this train by a pulse picker (PP)[3] and amplified in a multi-pass flash lamp pumped Nd:glass laser cavity. The output of the multi-pass amplifier is further amplified in two 2-pass Nd:glass amplifiers. The frequency of the IR pulse is then doubled and quadrupled to the UV ($\lambda = 263.5$ nm), in two 10 mm BBO crystals. Finally the UV pulse is transported to the cathode at a distance of 20 m from the laser room. The laser parameters are summarized in Table 1. Presently, up to 800 pulses spaced at 1 μs can be delivered at a repetition rate of 1 Hz.Information on a similar laser system installed at the TESLA test facility at the DESY laboratory in Hamburg, Germany, can be found in Refs. [4,5].

An important precondition for successful operation of the photoinjector is a stable and reliable laser that delivers UV laser pulses conforming to the requirements of the linac. The first version of the drive laser was installed in 1998 [6] and has been in operation since then, but was limited in certain aspects. Most seriously, the chirp of the seed pulse, generated by group velocity dispersion (GVD) in a 2 km long fiber, was unstable due to environmental fluctuations. The compression ratio of the grating

---

*Corresponding author. 2025 NW Cornelius Pass Rd., Hillsboro, OR 97124, USA. Tel.: 585 414 7028; fax: 503 547 6017.
E-mail address: jlli@synopsys.com (J. Li).

0168-9002/$ - see front matter © 2006 Elsevier B.V. All rights reserved.
doi:10.1016/j.nima.2006.04.032

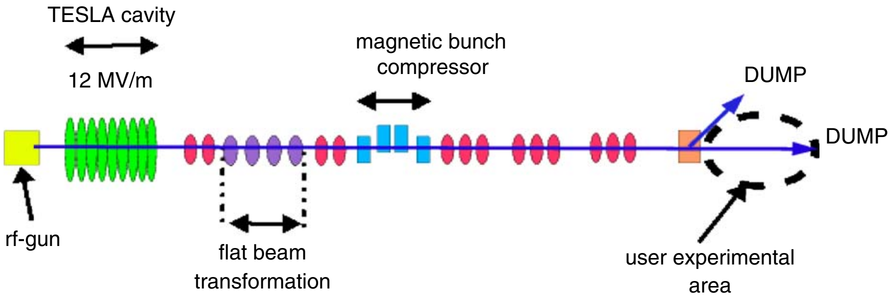

Fig. 1. Schematic overview of the photoinjector at A0.

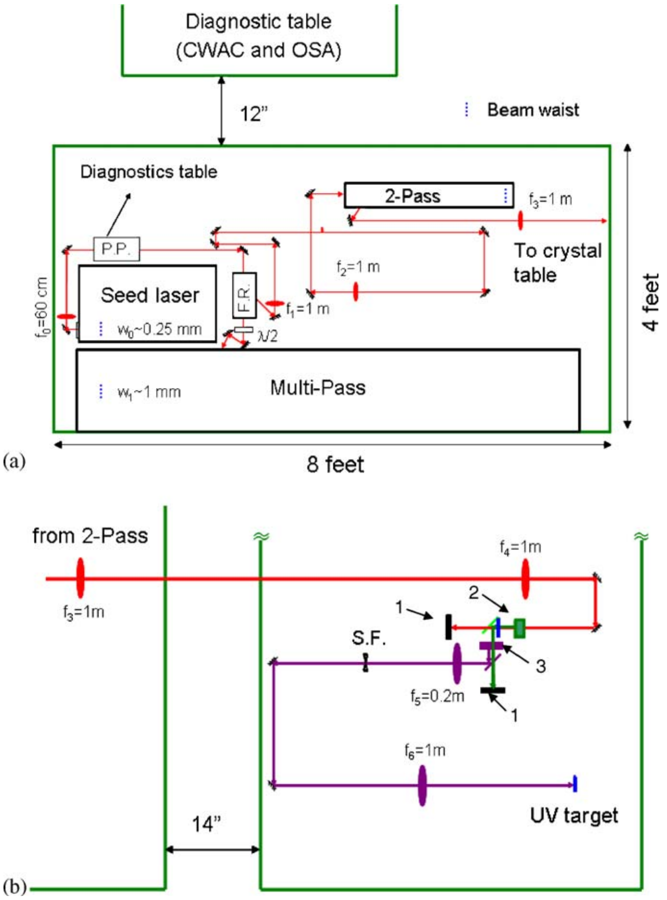

Fig. 2. Layout of the laser system, amplifier table (a) and crystal table (b). PP designates a Pulse Picker; FR, Faraday Rotator; 2P, two-pass amplifier; SF, spatial filter; 1, beam dump; 2, 10 mm doubling BBO crystal; 3, 10 mm quadrupling BBO crystal.

Table 1
Laser parameters

Oscillator frequency	81.25 MHz
Oscillator wavelength	1054 nm
Oscillator energy/pulse	5.5 nJ
Energy/pulse after multi-pass	6 μJ
Energy/pulse after two-pass	100 μJ
UV energy/pulse after crystals	20 μJ
UV energy/pulse on cathode	10 μJ
UV pulse length (FWHM)	5 ps
Separation of pulses in train	1 μs
Length of pulse train	up to 800 pulses
Repetition rate	1 Hz

compressor consisting of a pair of gratings, in a fixed configuration, is dependent on the chirp of the input beam, and hence, the output pulse duration was unstable. Such pulse length instability turns into amplitude fluctuations when the frequency of the IR beam is doubled and quadrupled. Furthermore, it was difficult to maintain optimal coupling of the seed pulse into the multi-pass amplifier, requiring the use of a large number of round trips (as many as 13) to achieve the desired gain. As discussed later this contributes significantly to shot-to-shot fluctuations. The absence of image relay in the optical system degrades the wavefront, resulting in decreased efficiency during frequency conversion. It also made it difficult to control the profile of the UV on the cathode. In the newly upgraded system the above problems have been resolved.

In the following sections, we discuss the individual components as well as the overall performance of the laser system. We begin by describing the characterization of the new seed laser. In the third section, we present details on the amplification of the seed pulse in the multi-pass and 2-pass amplifiers. We also discuss the image relay optics, designed to preserve the beam waist and maintain the beam transverse profile. The IR beam waist is relayed to the doubling and quadrupling crystals so that the wavefront at the crystals is flat. The quality of the UV beam was improved by introducing a spatial filter inserted at the focal point of the UV telescope.

The final section is divided into several subsections that cover different aspects of the system's performance. We first discuss shot-to-shot fluctuations. By comparing the amplitude fluctuations after the multi-pass amplifier and in the UV, we conclude that the primary source of the fluctuations is the instability of the power supply driving the flash lamp of the multi-pass amplifier. The transverse and longitudinal profiles of the UV beam, which were measured using, respectively, a CCD camera and a streak camera are presented. We also describe the UV pulse stacker and the transport line to the photocathode. Four UV pulses were stacked with a fixed time delay to construct